

Section 5

Biological Modeling

Section Editor: Nathan Baker

Pacific Northwest National Laboratory, Richland, WA 99352, USA

Modeling Signaling Processes across Cellular Membranes Using a Mesoscopic Approach

George Khelashvili¹ and Daniel Harries²

Contents		
	1. Introduction	238
	1.1 Lipid rafts as platforms for cellular signaling	238
	1.2 The need for large-scale quantitative models to describe complex signaling machinery	239
	2. Mesoscopic Model of Membrane-Associated Signaling Complexes	240
	2.1 Overall strategy	240
	2.2 System representation and governing free energy	241
	2.3 Free energy minimization	244
	2.4 Quantitative description of peripheral protein diffusion	245
	2.5 Accounting for amphipathic helix insertions	246
	3. Model Applications	246
	3.1 PIP ₂ and cellular signaling—mechanisms of membrane targeting	246
	3.2 BAR–membrane interactions	248
	3.3 Adsorption of natively unstructured protein domains onto lipid membranes	252
	4. Future Prospects	256
	Acknowledgments	257
	References	257

Abstract Computational models are effective in providing quantitative predictions on processes across cellular membranes, thereby aiding experimental observations. Conventional computational tools, such as molecular dynamics or Monte Carlo simulation, offer significant insights when applicable. However, it remains extremely difficult to use these simulation methods to describe large

¹Department of Physiology and Biophysics, Weill Medical College of Cornell University, New York, NY, USA

²Institute of Chemistry and the Fritz Haber Research Center, The Hebrew University of Jerusalem, Jerusalem, Israel

macromolecular assemblies within timescales relevant to a vast majority of critical physiological processes. To overcome this outstanding challenge, alternative methods based on coarse-grained representations have more recently emerged. In this chapter, we review one such particular advanced methodology that is based on mean-field-type representations typically used for equilibrium thermodynamic calculations of lipids and proteins. The main advantages of this self-consistent scheme are in adding information concerning longer timescales and in gaining access to the steady state of the system without making a priori assumptions concerning protein–membrane interactions. We illustrate this methodology using several examples pertaining to interactions of peripheral signaling proteins with lipid membranes. These examples outline the current state of the computational strategy and allow us to discuss several future enhancements that should help the scheme become a powerful methodology complementary to other simulation techniques. With these extensions, the proposed methodology could enable quantitative description of large-scale membrane-associated interactions that are of major importance in physiological processes of the healthy and diseased cell.

Keywords: cell signaling; lipid rafts; BAR domains; membrane curvature; membrane elasticity; PIP₂ diffusion; mean-field model; coarse-grained theory; Poisson–Boltzmann theory; Cahn–Hilliard equations

1. INTRODUCTION

1.1 Lipid rafts as platforms for cellular signaling

Overwhelming evidence indicates that function and organization of protein components of living cell membranes are orchestrated at specific spatial and temporal scales. In particular, structural, compositional, and mechanistic properties of lipid bilayers play a significant role in regulating the physiological function of membrane-associated proteins [1]. One of the best known examples is the existence of specialized plasma membrane domains, typically enriched in cholesterol and sphingolipids. These patches, termed “rafts”, have been implicated as platforms for various physiological processes, and specifically for cellular signal transduction [2].

As such, rafts have been shown to be important in regulating the function of both transmembrane (TM) and peripheral signaling proteins. For instance, evidence suggests that cholesterol-dependent separation of the TM signaling G-protein-coupled receptors (GPCRs) from their partners can be a determining factor for signaling efficacy [3]. Another example is the use of polyvalent phosphatidylinositol 4,5-bisphosphate (PIP₂) lipids, also found to be enriched in rafts, for membrane targeting by various peripheral signaling motifs, such as C2 [4], PH [5], FERM [6], and BAR domains [7]. BAR domains present a particularly fascinating case because they have been found to act as mechanistic modules that are capable of locally reshaping plasma membranes as a part of cell signaling and other physiological functions such as endocytosis [7]. Importantly, BAR modules are involved synergistically with other protein domains, such as PDZ domains, in

interactions with GPCRs to direct subsequent steps in signaling through their effects on membrane remodeling. While this synergism has been proposed specifically for those proteins interacting with C-kinase 1 (PICK1) [8], the abundance of BAR domain containing proteins highlights the importance of this class of mechanisms and their putative physiological roles.

A fundamentally important question for the role of rafts in cellular signaling is whether such domains exist preformed in living cells so that they can be recognized by the cellular protein machinery, or alternatively, could rafts present structures that dynamically assemble, adopting specific lipid composition or membrane deformations around specific protein components in response to physiological function [2]. Biochemical and biophysical studies conducted *in vitro* on cell membranes, as well as on model lipid assemblies, established that rafts can exist as stable membrane domains in the liquid-ordered (L_O) phase surrounded by a relatively fluid (L_α) lipid environment (for example, see References [9–14] and references therein). These domains are physically different both structurally and mechanistically from the surrounding lipid matrix. In particular, rafts are generally thicker and more rigid compared to other membrane compartments [15–19]. These studies also identified additional putative raft components, such as glycosylphosphatidylinositol (GPI)-anchored proteins or TM domains [20,21]. However, despite the wealth of data collected *in vitro*, the challenge in the field still remains to link structural and mechanistic raft characteristics observed in artificial systems with those in living cell membranes under native conditions, where language borrowed from macroscopic phase transitions may become inadequate [2,16].

1.2 The need for large-scale quantitative models to describe complex signaling machinery

The difficulty with realistically describing rafts and associated interactions during signal transduction originates from the large number of concerted actions involved. When signaling proteins and other macromolecules adsorb, diffuse on cell membranes, penetrate into the membrane, and associate/dissociate in complexes within the membrane, they interact through intricate forces that ultimately determine biological function. This complexity of interaction makes it conceptually challenging and computationally very costly to quantify such encounters at the macromolecular level.

Computational models are powerful in aiding experimental observations by providing quantitative, testable predictions. However, while conventional computational tools, such as molecular dynamics (MD) or Monte Carlo (MC) simulations, offer significant insight when applicable, it remains very difficult to use them in order to describe large macromolecular assemblies within timescales relevant to a vast majority of critical biological processes. Even if the required force-fields are available, using current supercomputational resources, it is possible in exceptional cases to use MD simulations for ca. 1 μ s for systems as large as 250,000 atoms. But even these relatively extended size and timescales do not permit the consideration of processes that include membrane reshaping, lipid

reorganization, and protein–protein interactions, which evolve concertedly at the lipid membrane interface.

Not surprisingly, methods have been devised in sustained efforts to address this perennial challenge. Recent computational strategies have attempted to coarse-grain the system, thus lowering the number of degrees of freedom addressed by the model, thereby also reducing the required computational effort (see, e.g., References [22–25]). However, most of these strategies rely on designing force-fields for specific mesoscopic models, a formidable task in itself.

We have been pursuing a somewhat different approach, which takes advantage of the extensive knowledge and quantitative information accumulated on lipids, proteins, and their interactions. In particular, to model membrane-associated interactions during cellular signaling, we take advantage of available information on the elastic, entropic, and electrostatic properties of lipids and proteins [26,27]. Our starting point is mean-field-type theories that are typically used for equilibrium thermodynamic calculations of lipids and macromolecules such as proteins. Information resulting from these models is then fed as inputs to dynamic Cahn–Hilliard (CH) and stochastic Langevin formulations [28] that allow probing of the molecular interactions of membrane-associated proteins in time and space. With this algorithmic formulation, we concentrate on explicitly describing only a smaller number of important degrees of freedom, precluding the need to model individual lipid components.

In this review, we describe our modeling strategy and present several applications of the method. All the considered examples relate to interactions of peripheral signaling motifs, such as BAR domains or basic (hence positively charged) polypeptides with membranes of raft-like lipid compositions. We aim to illustrate the effectiveness of our approach in describing dynamic membrane processes that involve membrane remodeling upon protein adsorption, as well as lipid rearrangement and segregation following their interaction with adsorbing proteins.

The main advantages of this self-consistent scheme are in adding information concerning longer timescales and gaining access to the steady state of the system without making a priori assumptions on protein–membrane interactions. We end by discussing future perspectives and possible extensions of the model that will hopefully allow this to become a powerful methodology complementary to other simulation techniques, such as MD. Together, these strategies should enable the study of large-scale membrane-associated interactions that are of major importance in physiological processes of the cell in both healthy and diseased states.

2. MESOSCOPIC MODEL OF MEMBRANE-ASSOCIATED SIGNALING COMPLEXES

2.1 Overall strategy

We start by discussing our overall strategy to coarse-grain macromolecular representations by using available information from experiments and from results of atomistic simulations on the material properties of proteins, membranes, and lipid

components, as well as their interactions. This information can be used in order to devise models that treat explicitly only a smaller number of important degrees of freedom. Thus, to quantify the combined kinetic effect of many lipid species interacting with peripheral proteins, and to describe the concomitant membrane shape perturbations, it is essential to be able to calculate the steady state of adsorbing macromolecules in a way that will include all important degrees of freedom in a self-consistent manner. These interactions include electrostatics (Coulomb) forces, lipid mixing, and membrane elastic deformations. In our formulation, self-consistency is achieved by minimizing the governing model free energy density functional, which is based on the continuum Helfrich free energy for membrane elasticity [29], and on the nonlinear Poisson–Boltzmann (PB) theory of electrostatics [30–34]. By providing a realistic three-dimensional treatment of the electrostatic problem, and requiring only a few phenomenological material constants to describe the lipid bilayer, this simple formalism accounts for a number of important membrane properties. Although this mesoscopic theory neglects most atomic structural features of a lipid bilayer [34,35], similar membrane and membrane–macromolecule models have been shown to yield reliable qualitative and quantitative predictions [36–47].

2.2 System representation and governing free energy

Our method uses an atomic-level representation of the adsorbing protein in three dimensions, and accounts for lateral reorganization and demixing of lipids, as well as membrane deformations upon adsorption (see Figure 1). We consider the limit of low surface density of adsorbing proteins, so that interactions between

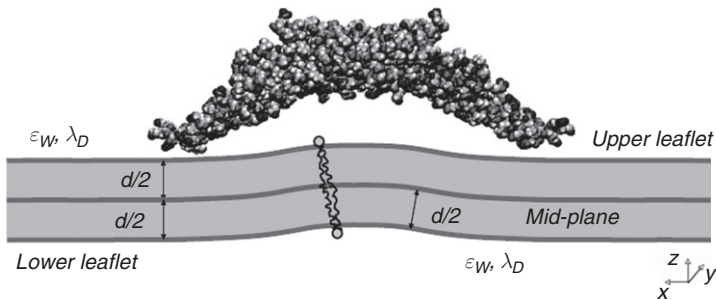


Figure 1 View of the BAR–membrane complex at steady state, as predicted from coarse-grained mean-field-level calculations. BAR is shown in spacefill; the membrane interior is shaded gray. In this hybrid model, BAR domain is represented in its all-atom detail, through partial charges and the radii of each constituent atom. The membrane is represented as a two-dimensional incompressible, tensionless, elastic medium comprised of 2D smooth charged surfaces (where the lipid polar head-groups reside), and a low-dielectric hydrophobic core volume. Elastic properties of the membrane are characterized by its bending modulus and locally defined spontaneous curvatures. The system is driven toward equilibrium through the self-consistent minimization of the free energy functional, the latter containing contributions from the system’s electrostatic energy, mixing entropy of lipids and ions in the solution, and membrane deformation energy.

proteins are negligible. The adsorbing protein is represented in full-atomistic 3D details, whereas the membrane is considered as a two-dimensional fluid, allowing us to treat lipid head-group charges in the continuum representation, as usual in regular solution theory.

For simplicity of presentation, we assume here membranes containing binary mixtures of acidic and neutral (zwitterionic) lipids. The temporal evolution of the spatially varying charged-lipid compositions on the membrane upper (u) and lower (l) leaflets are linked to the Laplace–Beltrami (LB) operators acting on the corresponding electrochemical potentials through two CH equations (one for each leaflet) each of the form [28]:

$$\frac{\partial \phi(\vec{r}, t)}{\partial t} = D_{\text{lip}} \nabla_{\text{LB}}^2 \mu(\vec{r}, t) = \frac{D_{\text{lip}}}{\sqrt{g}} \partial_i \left(\sqrt{g} g^{ij} \partial_j \mu(\vec{r}, t) \right) \quad (1)$$

Here, ϕ and μ denote respectively the local mole fraction and local electrochemical potential of the charged lipid species in that particular leaflet, g is the metric tensor defined on the leaflet surface, and D_{lip} represents the diffusion coefficient of charged lipids. Note that D_{lip} should not affect the equilibrium state. The local electrochemical potentials, in turn, are derived from the free energy functional that itself depends on local lipid component densities ϕ and membrane curvature. This property results in a self-consistent formulation, which remains as the main computational task.

More specifically, we assume that the system's free energy F consists of electrostatic energy, mobile salt ion translational entropy, lipid mixing entropy contributions, membrane bending energy, and a short-range repulsive interaction energy acting between protein and membrane interfaces [26,27,36,43,44]:

$$F = F_{\text{el}} + F_{\text{IM}} + F_{\text{lip}} + F_{\text{b}} + F_{\text{rep}} \quad (2)$$

The system's electrostatic (Coulomb) energy is given by

$$F_{\text{el}} = \frac{1}{2} \varepsilon_0 \left(\frac{k_B T}{e^2} \right) \int_V \varepsilon_d (\nabla \Psi)^2 dV \quad (3)$$

Here, $\Psi = e\Phi/k_B T$ is the dimensionless (reduced) electrostatic potential, with Φ representing the electrostatic potential, k_B the Boltzmann's constant, T the temperature, and e the elementary charge; ε_0 is the permeability of free space, while ε_d is the dielectric constant within the volume element dV . We take ε_d as 2.0 inside the membrane and the protein and as 80.0 in the aqueous solution. The integration in Eq. (3) is performed over the volume V of the entire space.

The contribution from the translational entropy of mobile (salt) ions in solution is

$$F_{\text{IM}} = k_B T \int_V \left[n_+ \ln \frac{n_+}{n_0} + n_- \ln \frac{n_-}{n_0} - (n_+ + n_- - 2n_0) \right] dV \quad (4)$$

where n_+ and n_- are local concentrations of mobile cations (+) and anions (-), respectively, and n_0 is the electrolyte concentration in the bulk.

The contribution from the 2D mixing entropy due to the mobile lipid molecules within each leaflet is

$$F_{\text{lip}} = \frac{k_B T}{a} \int_{A_u} \left[\phi_u \ln \frac{\phi_u}{\phi_u^0} + (1 - \phi_u) \ln \frac{(1 - \phi_u)}{(1 - \phi_u^0)} \right] dA_u + \frac{k_B T}{a} \int_{A_l} \left[\phi_l \ln \frac{\phi_l}{\phi_l^0} + (1 - \phi_l) \ln \frac{(1 - \phi_l)}{(1 - \phi_l^0)} \right] dA_l \quad (5)$$

These integrals represent entropic penalties associated with lipid demixing due to possible lipid segregation, on the upper and the lower surfaces of the membrane, respectively. In Eq. (5), ϕ_u^0 and ϕ_l^0 denote the average compositions of charged lipids on the respective leaflets, and a represents the area per lipid head-group.

The membrane bending energy in Eq. (2) is the sum of local elastic energies associated with deformations of individual membrane leaflets away from their spontaneous curvatures, as described by the Helfrich free energy:

$$F_u = \frac{1}{2} \kappa_m \int_{A_u} (c_u - c_u^0(\phi_u))^2 dA_u + \frac{1}{2} \kappa_m \int_{A_l} (c_l - c_l^0(\phi_l))^2 dA_l \quad (6)$$

Here, c_u and c_l are the local mean curvatures of each of the two membrane monolayers, and κ_m denotes the bending rigidity of a single monolayer that is here assumed to be the same for each leaflet and for both lipid species. The spontaneous curvatures of the two leaflets, c_u^0 and c_l^0 are described as sums of the spontaneous curvatures of the pure lipid constituents weighted by their local compositions. This approximation has been previously validated [36,48].

Functionally minimizing F with respect to the compositional degree of freedom ($\delta F / \delta \phi = 0$) results in an expression for the (local) electrochemical potential for charged lipid species on each leaflet [27,36]:

$$\mu = \mu^0 + k_B T \left(\ln \frac{\phi(1 - \phi^0)}{\phi^0(1 - \phi)} + z\Psi \right) + a\kappa_m (c_n^0 - c_c^0)(c - c^0(\phi)) \quad (7)$$

where ϕ^0 is the average mole fraction of charged lipids, z denotes the valency of charged lipid species, and c_n^0 and c_c^0 represent the spontaneous curvatures of the pure neutral and charged lipids, respectively. Adding lipid species to the formulation is straightforward, and simply involves modifying the free energies to include an additional compositional variable.

Finally, the short-ranged repulsive term F_{rep} accounts for the energy contribution related to excluded volume and hydration forces that appear when two surfaces (protein and membrane) come into close proximity of each other [49–52]. This term in the free energy functional is taken as a hard wall potential

that restricts membrane–protein minimal approach to be $\geq 2 \text{ \AA}$, and excludes any configuration that violates this limitation.

2.3 Free energy minimization

The free energy functional in Eq. (2) must be minimized with respect to all relevant degrees of freedom in a self-consistent manner. In particular, functionally minimizing F with respect to the mobile ion concentrations leads to the familiar nonlinear PB equation [26–36]:

$$\nabla^2 \Psi = \lambda^{-2} \sinh \Psi \quad (8)$$

where $\lambda = (\varepsilon_0 \varepsilon_w k_B T / 2e^2 n_0)^{1/2}$ is the Debye length. This equation is typically used to describe electrolyte solutions at the mean-field level. Solving Eq. (8) for the volume occupied by the aqueous solution yields the reduced electrostatic potential Ψ in space. Note that Ψ , in turn, is linked to local lipid compositions in each leaflet through the boundary condition on the leaflet surface $\partial \Psi / \partial r = -ez\phi / (a\varepsilon_0 \varepsilon_d)$, where z and a are valency and lateral area per head-group of charged lipids, respectively.

Using the expression for the chemical potential Eq. (7) together with the nonlinear PB Eq. (8) for electrostatic potential and the CH Eq. (1) that describes the temporal evolution of the system from any arbitrary (nonequilibrium) state, the total free energy can be minimized with respect to the local lipid compositions [53–55]. Practically, this is done by following the state of the system at long times, where steady state is reached. One tacit assumption behind our minimization strategy is that lipid diffusion is fast enough so that lipid compositions locally and continuously adapt to the electrostatic potential in space emanating from the macromolecular adsorbate.

In fact, F is also required to be at a minimum with respect to all possible membrane deformations, and this minimization with respect to membrane shape must be carried out self-consistently together with the electrostatic and lipid mixing contributions [27,36]. This presents a challenge, since in principle one has to consider all possible variations in membrane geometry, and these multiple shape deformations generally couple to other degrees of freedom.

To overcome this problem, we have designed a novel combined scheme that efficiently accounts for bilayer deformations together with the electrostatic PB solution self-consistently [27]. Our strategy is based on representing the membrane interface shape (contour) as a linear superposition of N Gaussian functions (used here as a basis set) centered at different locations on the surface of the membrane. In this manner, we can approximate the local membrane height $h(x, y)$ at any point (x, y) by the following sum [27]:

$$h(x, y) \approx \sum_{i=1}^N A_i \times \exp \left[- \left(\frac{(x - x_i^0)^2}{\sigma_{x_i}^2} + \frac{(y - y_i^0)^2}{\sigma_{y_i}^2} \right) \right], \quad (9)$$

where A_i -s and σ_i -s denote the amplitude and variances of the i th Gaussian centered at (x_i, y_i) . With that, we sample membrane deformations by varying only the Gaussian amplitudes. Note that, A_i -s and σ_i -s are coupled to local membrane curvature through the relation $c = \nabla_{\text{LB}}^2 h(x, y)$, while this local curvature itself is linked to the local lipid composition ϕ as described in Eq. (6).

The described minimization procedure significantly reduces the dimensionality of phase space that needs to be explored. In the minimization procedure, different Gaussian's amplitudes are varied at random, and trial moves are accepted only if following the move the free energy is reduced. To ensure self-consistency, at each trial move we also solve the appropriate PB equation to obtain the electrostatic potential for the particular membrane shape. To couple shape changes to lipid mixing, we alternate between steps aimed at varying membrane deformations, with CH moves that spatially propagate local lipid compositions. This procedure allows the solution to converge to the (local) minimum of the total free energy.

2.4 Quantitative description of peripheral protein diffusion

To also follow the diffusion of an adsorbed protein on a membrane interface, our method implements a dynamic Monte Carlo (DMC) scheme [56–62]. This procedure is advantageous in that it directly relies on available free energies and does not require additional force calculations, which can be time-consuming. According to this scheme, the adsorbed protein diffuses on the membrane surface tracing a stochastic dynamic trajectory. This probabilistic path is generated in accordance with the fluctuation–dissipation theorem, as the adsorbent's center of mass makes random displacements in the two directions of the membrane plane each of size $\alpha\sqrt{2\Delta t'D'}$, where α is a Gaussian random number with zero mean and unit variance, $\Delta t'$ denotes the dimensionless time-step, and D' represents the ratio of protein to lipid diffusion constants [26]. The random trial move is then accepted or rejected according to a Metropolis-like criterion employing the usual transition probability W of value

$$W = 1 \quad \text{if} \quad F_{\text{new}} = F_{\text{old}}, \quad \text{and} \quad W = e^{-(F_{\text{new}} - F_{\text{old}})/k_B T} \quad \text{if} \quad F_{\text{new}} > F_{\text{old}} \quad (10)$$

Here, F_{old} and F_{new} are, respectively, the adsorption free energies of the “old” state (before the trial move) and “new” state of the protein–membrane system. If a trial move is accepted, the macromolecule is advanced to the “new” position, the CH equations for lipids are solved, and sampling of membrane deformations are performed for the newly accepted position of the adsorbate. If, on the other hand, the trial move is rejected, the protein remains at its previous position, and the same minimization step is conducted, only now with respect to the previous “old” location of the adsorbate.

2.5 Accounting for amphipathic helix insertions

An additional important force that should be considered corresponds to the effect of protein amphipathic helix membrane insertions that often play a critical role in attracting proteins to lipid membranes and in generating membrane curvature (see below). We have made use of an implicit representation of this effect by defining a membrane area (patch) of positive spontaneous curvature (defined as curving “toward” the adsorbing protein) that forms directly “under” an adsorbing protein at the interaction zone. We then use a phenomenological approach that assumes that the inclusions perturb the bilayer symmetry and its elastic properties primarily around the area of helical insertion [63,64]. We account for insertions to different membrane depths by varying the value for the spontaneous curvature assigned to this locally perturbed membrane region. For each insertion depth, the bilayer is allowed to adjust its geometry locally. The corresponding deformations at steady state for each penetration depth is found by minimizing the modified free energy functional, which now contains an additional (elastic) free energy term accounting for the nonzero spontaneous curvature region near the adsorbed protein.

3. MODEL APPLICATIONS

3.1 PIP₂ and cellular signaling—mechanisms of membrane targeting

In this section we present several model applications pertaining to the role of polyvalent PIP₂ lipids in membrane targeting of peripheral proteins. This targeting mechanism is of special interest for the link between cellular signaling and lipid rafts, because among their multiple functions, PIP₂ lipids are known to act as scaffolds for the recruitment of proteins with specific binding domains toward special cell membrane regions, namely rafts, during signal transduction [65]. Through this mechanism, PIP₂ lipids are thought to precisely regulate cell signaling both temporally and spatially.

Many of the architectural signaling proteins that use PIP₂ lipids for membrane targeting contain structured domains, through which specific binding to polyvalent lipids is achieved. Examples include the C2 [4], PH [5], FERM [6], and BAR domains [7]. However, an apparently different type of targeting is realized by numerous other proteins that contain natively unstructured clusters of basic residues, such as the well-studied examples of the GAP43, GTPase K-Ras, and MARCKS proteins or peptides [66–70]. Below, we describe our model application to both structured and unstructured protein domains interacting with PIP₂-containing membranes.

The use of positively charged residues for targeting may come as no surprise, as cellular plasma membranes typically contain ~20% anionic lipids. This affords a simple mechanism for protein–lipid binding that is essentially nonspecific, yet able to confine proteins to membrane interfaces. This simple molecular picture has been challenged by recent theoretical and experimental evidence suggesting

that the major anionic lipid component in many cells, phosphatidylserine (PS) (or phosphatidylglycerol), might not be the major participant in peripheral protein binding. Instead, polyvalent lipids such as PIP_2 are more likely implicated in segregation close to peripherally adsorbed proteins [45,71–73]. Despite the fact that phosphoinositides constitute typically only around 1% of membrane composition [65], these minority lipids can act at sites of regulation at least partly by electrostatic association with peripheral and embedded proteins. Concentrating PIP_2 at the site of protein adsorption is therefore a likely mechanism for local and specific recruitment. It has been suggested that segregated lipids can subsequently be released upon cellular changes, e.g., in Ca^{2+} concentrations. This provides a way to control the amount of free PIP_2 in the membrane, and hence a mechanism for regulating PIP_2 known to participate in cellular signaling processes such as enzyme activation, endocytosis, and ion-channel activation [74].

To begin to understand why electrostatic targeting could primarily be achieved by polyvalent rather than the more abundant monovalent lipids, one must focus on the forces that underlie this protein–lipid interaction. Experiments have suggested that PIP_2 preferentially segregates at sites of charged protein adsorption. This is reasonable because multivalent lipids should incur a smaller lipid demixing penalty and larger counterion release entropy [75–78] per segregated lipid, simply because each of them carries a larger charge. Recent theoretical studies predict that multivalent lipids should indeed segregate more than monovalent ones, and that the binding free energy to rigid macromolecules as well as to polyelectrolytes is significantly stronger for such lipids [45,72,73].

But recognizing the dynamic nature of the adsorption problem raises the possibility that the kinetic energy of each adsorbing protein allows it to move so quickly on lipid membranes that some lipids rarely manage to segregate at all. Conversely, lipids may rearrange so quickly around an adsorbing protein that the protein appears stationary to them, creating a transient “binding site”. The result can be a dynamic assembly of a domain or “lipid raft” around a peripheral, adsorbed protein. Through association with the protein, this raft could then impede the protein’s motion in the membrane plane.

Our mean-field theory provides an opportunity to quantitatively approach this problem, and describe the combined kinetic effect of many lipid species interacting with peripheral proteins. As described in the next sections, our model allows us to conclude that it is the composition of the membrane on which the adsorbed proteins are diffusing that sensitively determines whether lipids will be effectively sequestered. The model predictions also suggest that protein domains that selectively target PIP_2 -containing membrane regions can achieve such selectivity through electrostatic interactions alone, and without the need for any additional energy source. However, we also predict that, in order to deform spontaneously flat membrane patches, as required for physiological function, these proteins will utilize alternative mechanisms, such as amphipathic helix insertions. The role of electrostatics in this case appears to be the stabilization of locally deformed membrane structures, induced by amphipathic inclusions.

3.2 BAR–membrane interactions

As a first application example, we discuss the interactions of BAR domains with membranes. BAR domains have gained great interest in the study of cell physiological processes [79–81]. They are known to dimerize into a banana-like molecular structure [82] that adsorbs to and faces lipid membranes with its concave surface (see Figure 1). The interactions of BAR domain dimers with the cell membrane are associated with a curving of the interface regions that often contain a relatively higher concentration of negatively charged lipids [7,83–85]. The functional role of such membrane remodeling by BARs apparently is to cluster and localize proteins in specialized membrane regions, and is likely to be important for signaling [8]. When present at high concentrations, BAR is capable of tubulating and vesiculating lipid membranes both in vivo and in vitro [8,86]. Some BAR domains (termed N-BARs) have N-terminal regions that appear to fold into amphipathic helices upon BAR–membrane binding, and to insert into the polar head-group region of lipid membranes [86–95].

3.2.1 Elements of membrane remodeling by BAR domains

In transforming a membrane that is spontaneously flat at equilibrium into a highly curved structure, BAR appears to take advantage of a special set of structural features (Figure 1). First, by pulling the membrane toward, or away from the protein, the electrostatic interactions between positively charged residues on BAR's concave surface and negative phospholipid head-groups may cause membrane deformations away from the flat bilayer plane. The same electrostatic interactions may also cause lateral sequestration of charged phospholipids near the protein [26,27,45–47,71–73]. This process of lipid demixing in the bilayer plane has been predicted to be particularly significant in membranes containing multivalent lipids, such as PIP₂ lipids [26,71,72]. Segregation of such highly charged lipids (net head-group charge of -4.0 at neutral pH [65]) would not only enhance the overall electrostatic interactions between BAR and membrane, but also lead to significant entropic gains. The entropic gain is due to the release into the bulk solution of mobile counterions that were previously bound to each of the macromolecule (protein and membrane) [75,77]. Furthermore, these membrane deformations could lead to local asymmetry between the spontaneous curvatures of the two monolayers comprising a lipid membrane, simply because the head-group of PIP₂ is larger than most monovalent lipids, such as PS, or zwitterionic lipids like phosphatidylcholine (PC). Such an asymmetry would be sufficient to produce a local positive curvature in the two *bilayer* leaflets toward the BAR [63,64,88].

Ultimately, sequestering charged lipids could potentially lead to a new stable state, in which bilayer bending forces favor membranes with local nonzero curvature. Moreover, the mechanism for coupling local lipid composition with membrane curvature may be complemented by a “local spontaneous curvature” mechanism [88], whereby the asymmetry between the spontaneous shapes of two monolayers is achieved by insertion of amphipathic N-terminal helices of certain BAR domains into the lipid polar head-groups region on one side of the membrane [7,88–95]. According to this mechanism, the insertion of an amphipathic

peptide into one of the leaflets of a flat membrane produces an increase in the local spontaneous curvature of that leaflet because of the local bending of the monolayer where the helix is embedded [63,64,88]. Differences in the spontaneous curvatures of the two monolayers comprising a lipid membrane, one with and the other lacking helical insertions, establishes a new equilibrium state, in which bilayer elastic forces support a locally curved membrane shape.

Application of the mean-field theory outlined in the previous section to BAR-membrane systems is geared specifically to discern the role of electrostatic interactions and amphipathic helix insertions in the process of membrane remodeling by BAR domains, by accounting for the coupling between electrostatically driven lipid sequestration and local membrane curvature. By bringing an energetic perspective to the problem, the model quantitatively answers the following critical questions: Can BAR-induced segregation of polyvalent PIP₂ lipids be the cause of substantial membrane deformation? And, how might N-helix insertions complement this coupling?

3.2.2 Lipid demixing upon Amphiphysin BAR dimer adsorption is insufficient on its own to induce significant membrane curvatures

Figure 2 shows a top view of the calculated lipid segregation and bilayer deformations for the equilibrium state of Amphiphysin BAR adsorbing on binary mixtures of 30:70 PS/PC and 4:96 PIP₂/PC that are compositionally symmetric on both membrane leaflets. In panel 2C, the BAR domain is outlined for clarity. The results of the free energy minimization procedure reveal weak membrane deformations at equilibrium under the influence of the adsorbing BAR for both PS- and PIP₂-containing membranes (Figure 2A–D). The largest membrane deformation, found in the center of the patches immediately under BAR's "arch", reaches only ~3–4 Å above the height of the planar membrane, a value comparable to the expected thermal undulations of the membrane at temperature $T = 300$ K and bending rigidity $\kappa = 20k_B T$ [97].

These insignificant membrane curvatures are accompanied by only minor segregation of charged lipid around the adsorbing protein in both bilayer mixtures (Figure 2E–H). Thus, even in the regions of strongest aggregation (*dark shades*) on the BAR-facing leaflet of the PIP₂-containing membrane, the PIP₂ lipid levels are elevated by only ~1.3 times their 4% bulk value. These PIP₂-enriched patches appear near the positively charged tips of the BAR domain, and their formation is the result of strong electrostatic interactions with negatively charged PIP₂ lipid head-groups. At the same time, the concentration of PS lipid on the BAR-facing leaflet is minimally affected by the BAR domain. Interestingly, the lipid demixing on the lower monolayer of both membranes can be explained entirely by bending forces acting where the membrane is negatively curved. This curvature favors regions depleted of PS and PIP₂ lipid (*lighter shades*) because these molecules have zero or even positive spontaneous curvature.

From the corresponding model binding free energy (ΔF) we can conclude that lipid demixing and membrane deformations contribute to a lowering ΔF for BAR/PS/PC and BAR/PIP₂/PC complexes by 1.9 $k_B T$ and 1.7 $k_B T$, respectively,

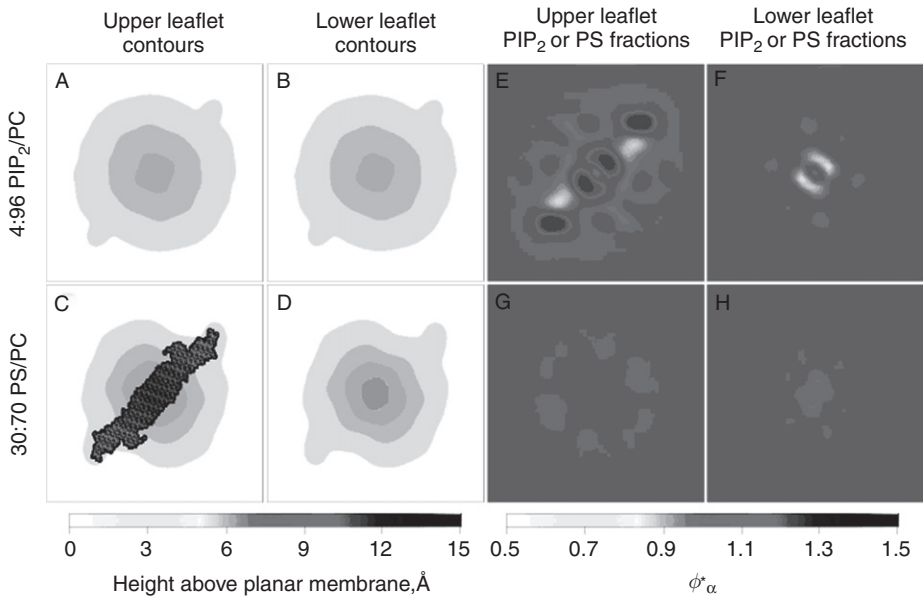


Figure 2 Adsorption of the Amphiphysin BAR domain on compositionally symmetric binary mixtures of PS/PC (*lower panels*) and PIP₂/PC (*upper panels*) lipid membranes. The membrane patches are characterized by bending modulus of $\kappa = 20k_B T$, and contain 0.3 and 0.04 fraction of PS and PIP₂ lipids, respectively. PS and PC lipids are described by spontaneous curvatures of $c_{PS}^0 = 1/144 \text{ \AA}^{-1}$, $c_{PC}^0 = -1/100 \text{ \AA}^{-1}$ [88]. The spontaneous curvature of PIP₂ is not known from experimental measurements. We assume here $c_{PIP_2}^0 = 1/70 \text{ \AA}^{-1}$ in light of the substantial difference in head-group size between PIP₂ and PS lipids. The BAR dimer orientation for both calculations is depicted in panel C as the projection of the BAR onto a membrane plane. Panels A–D show equilibrium membrane shapes of PIP₂/PC and PS/PC membranes, respectively, with contours shown for the local heights of the upper and lower leaflets. Panels E–H depict steady-state lipid distributions on the upper and lower leaflets of both membranes (ϕ_α^* , $\alpha = \text{PS, PIP}_2$). Shades for E–H panels represent ratios of local and average lipid fraction values. For all electrostatic calculations, we used a modified version of the APBS 0.4.0 software [96].

compared to the binding free energies of BAR onto the *flat* PS/PC and PIP₂/PC membranes of the same homogeneous compositions. Nevertheless, the combination of lipid segregation with the elastic forces within a membrane appears to be insufficient to produce significant compositional asymmetry between bilayer leaflets to drive significant bending deformations. Consequently, at steady state, the membrane remains near-flat, within fluctuations, upon BAR adsorption.

3.2.3 N-helix insertions can potentially enhance membrane deformations

In order to explore whether insertions of the BAR dimer's N-helices can enhance membrane curvature, various penetration depths of N-helices were examined, and the results are illustrated in Figure 3. We observe larger membrane deformations upon deeper insertion of N-helices (represented in the model by increasing the local spontaneous curvature). By performing quantitative analysis on binding

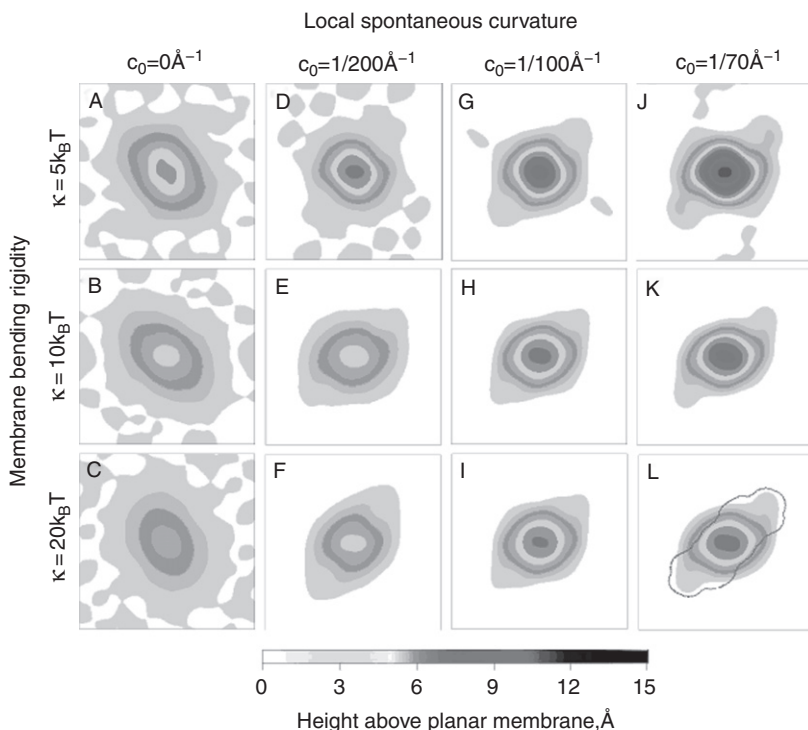


Figure 3 Steady-state shapes upon binding of the Amphiphysin N-BAR domain dimer plots show upper leaflet contours of membranes with different bending rigidities and with N-helix insertions of various depths. The membrane patches have -0.4 e/nm^2 average surface charge densities (corresponding to 0.3 PS lipid fractions) on both layers. The orientation of the BAR domain used in these calculations is the same as in Figure 2. For all systems, a nonzero spontaneous curvature c_0 domain was defined for a membrane patch inside the BAR projection area shown in panel L and extending 20 \AA away from the projected zone. The values for c_0 in the range of 0 – $1/70 \text{ \AA}^{-1}$ were used.

energies for the membrane patches shown in Figure 3, our model predicts that a single adsorbing Amphiphysin N-BAR dimer will stabilize membrane patches that have the inherent propensity for high curvature, reflected by the lipid tendency to create local distortions that closely match the curvature of the BAR dimer itself.

Additional calculations at different concentrations of charged lipids revealed that increasing PS lipid fraction from 0.3 to 0.5 resulted in stronger BAR binding with substantial (ca. $6k_B T$) strengthening of the adsorption free energy, but without noticeable changes in the equilibrium membrane deformation, shown in Figure 3. Taken together, the model results indicate that the N-helix insertions have a critical mechanistic role in the local perturbation and curving of the membrane, which is further stabilized by the electrostatic interaction with the BAR dimer.

Figure 3 is also a clear illustration that our method is able to accurately predict the experimentally observed and theoretically reproduced symmetry breaking

upon N-BAR dimer adsorption onto a membrane. Notably, our approach does so through the resulting self-consistent free energy minimization procedure, without a priori knowledge of any BAR-induced spontaneous curvature fields. This distinguishes our model from alternative mesoscopic approaches that assume BAR-generated nonisotropic curvature fields [25,98].

3.2.4 Membrane tubulation and vesiculation by arrays of BAR domains

A question that remains open is how the observed local deformations introduced by a single BAR translate into global changes in membrane shape observed upon binding of high concentrations of BARs [22,99–101]. Results of our calculations predict that, because of the interplay between electrostatic and elastic forces, a single BAR dimer deforms membranes so that the bilayer region under the BAR can be substantially curved. At the same time, the membrane remains flat within fluctuations beyond this interaction zone. Thus, it is clear that surrounding this high curvature area there must exist a narrow region, or “rim”, where the sign of the local membrane curvature changes from positive (under the BAR) to negative (outside the interaction zone) eventually decaying to zero. Although electrostatically advantageous, the formation of such a rim is opposed by bending forces within the membrane, because lipids in the rim zone pay an elastic penalty for bending away from the spontaneous curvature c_0 . The larger the membrane deformations, the larger the expected free energy penalty exerted on the rim. To conclude, binding of an additional BAR will be most favorable energetically if, together with minimizing the electrostatic interactions, the BAR also alleviates the membrane stress introduced by the one already adsorbed. The optimal manner for achieving this effect with multiple BARs is clearly not a simple additive superposition of effects from a single BAR, but rather must include collective properties [22,99–101]. Bridging the gap between our calculations and experimental results showing membrane tubulation and vesiculation by arrays of BAR domains is one of the future challenges in the field of BAR/membrane modeling.

3.3 Adsorption of natively unstructured protein domains onto lipid membranes

As an illustration of membrane binding of natively unstructured protein domains, we describe the predictions from our calculations pertaining to the adsorption of basic lysine-13 (Lys13) peptides onto mixed lipid membranes. Basic polypeptides, such as Lys13, are well-studied simple yet realistic models to describe membrane anchoring of unstructured domains such as MARCKS [46,71]. We first present results for stationary adsorbed Lys13 peptides in the presence of diffusing lipids. Then, to consider the effect of protein mobility, we discuss how our predictions change if the adsorbate is also allowed to diffuse.

3.3.1 Sequestration of PIP₂ lipids by adsorbing basic polypeptides

Figure 4 shows the charged lipid organization for a ternary 74:25:1 PC/PS/PIP₂ mixture (Figure 4a and b) and binary 71:29 PC/PS mixture (Figure 4c) upon

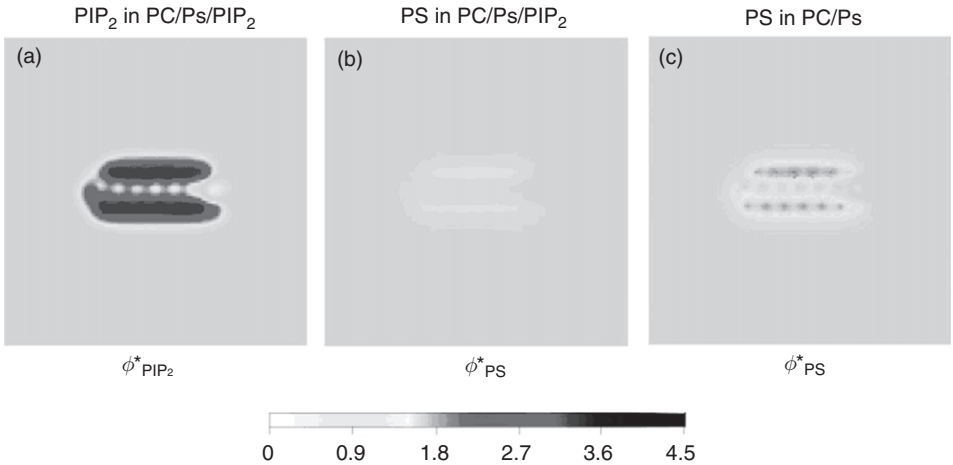


Figure 4 Adsorption of lysine-13 polypeptide onto ternary phosphatidylcholine (PC)/phosphatidylserine (PS)/PIP₂ lipid membrane with 74:25:1 composition (panels A and B), and onto binary PC/PS lipid membrane with 71:29 composition (panel C). (a) Normalized local fraction of PIP₂ lipids in the ternary system. (b) Local PS lipid fractions in the ternary system. (c) Local PS lipid fraction in the binary mixture. All plots shown for $t = 0.5 \mu\text{s}$ after beginning of propagation. For these calculations lysine-13 was placed near the membrane, such that the minimum distance between van der Waals radii of lysine-13 and membrane atoms was 3 Å, and the peptide was oriented with its major (long) axis parallel to the bilayer plane.

Lys13 binding. Both lipid compositions are characterized by the same surface charge density, and the snapshots are taken after 500 ns (a point where steady state is achieved for lipid compositions) starting from a completely homogenous lipid distribution.

From [Figure 4a](#) we learn that the fraction of PIP₂ lipid increases up to 4.5-fold near the adsorbed Lys13 side chains, where the positive charge is greatest. This area is surrounded by a region with lower PIP₂ content, showing only 2.5–3-fold increase in multivalent lipid fraction. Because the peptide backbone is rich in both positive and negative charges, there are only minor changes in PIP₂ content along the Lys13 backbone with respect to the bulk concentration. In contrast, [Figure 4b](#) reveals almost no sequestration of PS by the peptide. The highest increase in PS lipid is only 1.5-fold, observed, as expected, along the Lys13 side chains. For comparison, [Figure 4c](#) shows that even in PIP₂-free membranes, the segregation of PS lipids around Lys13 is marginal.

Thus, in agreement with other theoretical predictions [45,46], our model indicates that an adsorbing *stationary* basic peptide will sequester primarily PIP₂ lipids, and will only very weakly sequester PS lipids.

3.3.2 Diffusion of peripheral proteins on lipid membranes

The intriguing question that now arises is how the extent of PIP₂ sequestration by Lys13 peptide described above will change when considering a more realistic

scenario, where the adsorbate is also allowed to diffuse on the membrane surface. In particular, we focus on how the macromolecule diffusion rates are affected by the acidic lipids in the membrane, and how different lipids can influence the apparent protein diffusion rates.

To address these questions, we follow a simplified spherical macroion that is allowed to move concomitantly with lipid diffusion. To do so, we extend our model to include protein diffusion and performed CH-DMC (see Section 2.4) calculations. We studied the same mixed membranes considered in Figure 4, focusing on two typical cases. In the first, the model protein has a diffusion constant much larger than that of lipids in the unperturbed (bare) membrane, with a ratio $D' = 10$ between the two, while in the second, the diffusion constant is comparable to that of the lipids, and $D' = 2$ (see Eq. 10). As we show, these two scenarios lead to different lipid and protein diffusion characteristics.

3.3.3 Modeling a fast protein diffusing over PIP₂-containing versus PIP₂-depleted membranes

Following the time evolution of the system, depicted in Figure 5c, reveals significant local PIP₂ lipid segregation around the fast-diffusing protein as it moves over a ternary PC/PS/PIP₂ membrane. Quantitative analysis of protein diffusion rates predicts a prominent concomitant retardation in the macroion's movement. Due to lipid rearrangement, the adsorbate diffusion becomes confined, for a limited time, to an area rich in PIP₂. However, due to the model protein's high mobility compared to that of lipids, the adsorbate occasionally and temporarily escapes, leaving behind the multivalent lipid cloud that had segregated around it.

The free diffusion of the macroion does not last very long, because PIP₂ lipids quickly segregate again around the new protein position. This segregation is due to the large forces acting on the PIP₂ lipids by the electrostatic field emanating from the adsorbate. Essentially, the macroion diffuses and drags PIP₂ lipids along its way, while the PIP₂ units that are segregated retard the free diffusion of the protein. In contrast to the strong PIP₂ segregation, we found that PS segregation in the ternary mixtures is very weak, in accordance with our previous findings for the stationary peptide (Figure 4b).

We compare this diffusion process with the same rapid model protein diffusing on a binary PIP₂-depleted membrane containing only monovalent (PS) lipids (Figure 5a). Clearly, acidic (PS) lipids segregate around the macroion to a much lesser extent compared to the ternary mixture, resulting in low energetic barriers to adsorbate motion. Hence, the diffusion of the macroion here is less restricted compared to that seen for the ternary mixture.

3.3.4 Slow protein diffusing over PIP₂-containing versus PIP₂-depleted membranes

Diffusion of a slower model protein, $D' = 2$, on the same binary and ternary membranes (Figure 5b and d, respectively) shows qualitatively similar behavior to that observed for $D' = 10$. However, due to the lower mobility of the macroion, the acidic lipids have more time to effectively segregate near the adsorbate, and

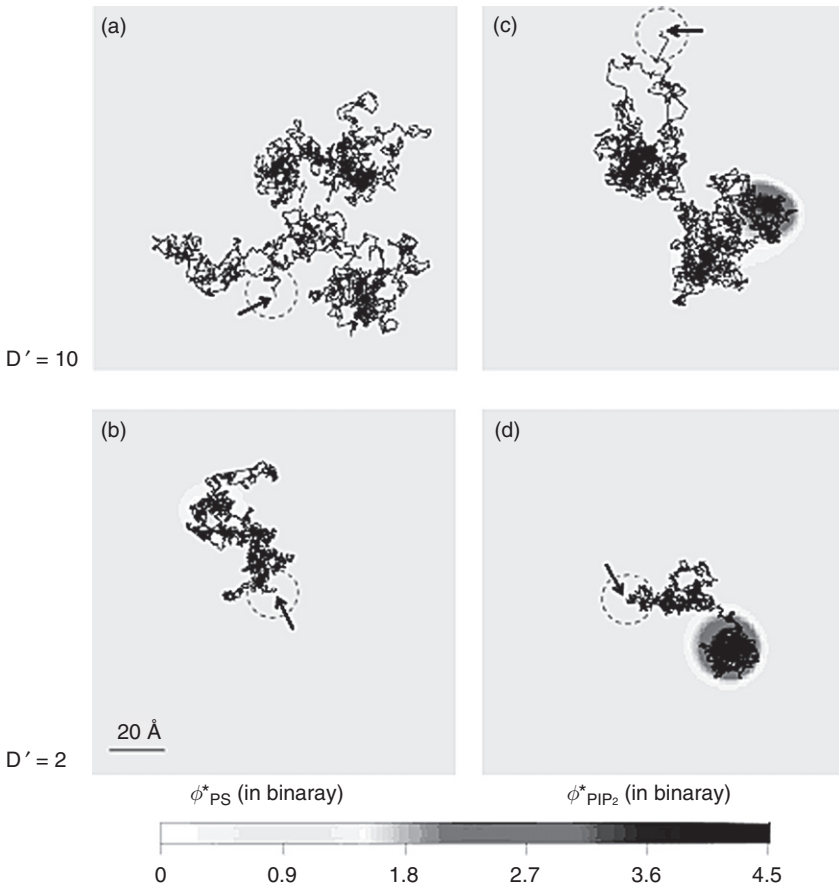


Figure 5 Diffusion of charged spherical macroion of radius 10 \AA and a uniform surface charge density of $1e^-$ per 93 \AA^2 on mixed membranes. The panels show the local surface charge densities after $0.6 \mu\text{s}$ of simulations (shades) and the entire macroion trajectories in that time (connected lines) for binary (71:29 PC/PS) mixture, $D'=10$ (a), for ternary (74:25:1 PC/PS/PIP₂) mixture, $D'=10$ (c), for binary (PC/PS) mixture, $D'=2$ (b), and for ternary (PC/PS/PIP₂) mixture, $D'=2$ (d). The dashed circles on each panel represent the projected size of the macroion with arrows indicating the starting position for the macroion center of mass. For clarity, the figures zoom on the relevant membrane surface region explored by the macroion, and a scale bar of 20 \AA is shown for reference.

therefore segregate more strongly. The result is that a majority of the macroion moves are restricted to the acidic lipid-rich patch that forms close to the protein. This is particularly noticeable for the ternary system, where the macroion practically never escapes to go beyond the circular patch formed by PIP₂ lipids, but rather diffuses together and within it. Whereas for the fast protein on ternary mixtures we observed the creation and destruction of macroion/PIP₂ “binding sites”, for the slower protein this lipid–protein “complex” stays intact for the entire trajectory. In a sense, we find that there are always PIP₂ lipids associated with the macroion as it diffuses on the membrane.

3.3.5 Implications for the role of PIP₂ in anchoring proteins to specialized membrane domains

Our results suggest that PIP₂ lipids can diffuse in concert with adsorbed molecules even when the diffusion of the adsorbate is much faster than lipid diffusion. In contrast, monovalent PS lipids segregate only weakly, so that macromolecule and lipid diffusion will remain largely uncorrelated. The difference in behavior between different lipid species arises because PIP₂ lipids, in the presence of the protein electric field, are much more mobile than PS, due to their higher charge and hence larger chemical potential.

Predictions from our model bear interesting implications for the role of PIP₂ lipids in anchoring natively unstructured domains (and other peripherally bound proteins) to lipid membranes. Clearly, to carry out their function, peripheral proteins must often remain localized in certain regions on the membrane (say, in rafts) for some duration of time. This requires a mechanism that would slow down diffusion across the membrane in the region in which these proteins must act. In agreement with recent experimental observations [70,71], our model predicts segregation of PIP₂ lipids around the diffusing charged protein, keeping these lipids effectively “bound” to the protein vicinity, and retarding the protein’s diffusive motion.

4. FUTURE PROSPECTS

We have presented a new computational modeling approach to describe membrane-associated interactions that evolve at mesoscales and over long times. Through illustrative examples, we showed how this self-consistent strategy is successful in elucidating some of the fundamental mechanistic aspects of cellular signaling. Specifically, we have shown how this method can not only help to discern the role of polyvalent lipids in recruitment and confinement of signaling proteins to specialized membrane regions to carry out their physiological function, but also can illuminate mechanisms responsible for membrane remodeling by signaling motifs such as BAR domains.

Toward developing a powerful and complete methodology, we are now pursuing several key enhancements and extensions to the model, to enable quantitative description of large-scale membrane-associated processes set in action by complex signaling machinery. Two major improvements are especially noteworthy in the context of lipid rafts and cell signaling. The first involves adding to the model quantitative details on TM protein–membrane interactions and connecting these degrees of freedom with the current knowledge on interactions between peripheral proteins and membranes. The second is to enable a description of phase separating elastic lipid membranes to capture the formation and dynamics of membrane rafts.

Obviously, these two enhancements are closely related through the well-known impact of cholesterol on both raft formation and functioning of raft-containing TM domains, such as GPCR proteins. Thus, with the intended modifications, the model should be able to elucidate the role of cholesterol and

other synergetic raft modulators in the function and organization of signaling proteins. With that, the extended methodology should become complementary to other simulation techniques, covering temporal and spatial regimes that are currently not readily accessible by existing techniques. The main gain for this type of approach (and a potential reason for the wider applicability) is that the method adds information concerning longer timescales and can reach the steady state of the system. Together with the opportunity to discuss protein-membrane interactions in terms of model free energies, the new methodology can, for the first time, begin to access a quantitative view of large-scale interactions during cellular signaling that act across the plasma membrane interface.

ACKNOWLEDGMENTS

We thank Nathan Baker, Michael Holst, and Todd Dolinsky for their advice on modifying the APBS code, as well as Harel Weinstein, Jim Sethna, Adrian Parsegian, David Andelman, and Brian Todd for valuable comments on the original manuscripts describing our method. GK is supported by grants from the National Institutes of Health P01 DA012408 and P01 DA012923. DH acknowledges support from the Israel Science Foundation (ISF Grant No. 1011/07) as well as an allocation for a high-performance computer cluster facility (ISF Grant No. 1012/07). The Fritz Haber research center is supported by the Minerva Foundation, Munich, Germany. Computational resources of the David A. Cofrin Center for Biomedical Information in the HRH Prince Alwaleed Bin Talal Bin Abdulaziz Alsaud Institute for Computational Biomedicine are gratefully acknowledged.

REFERENCES

1. McIntosh, T.J., Simon, S.A. Roles of bilayer material properties in function and distribution of membrane proteins. *Annu. Rev. Biophys. Biomol. Struct.* 2006, 35, 177–98.
2. Lingwood, D., Simons, K. Lipid rafts as a membrane-organizing principle. *Science* 2010, 327, 46–50.
3. Pontier, S.M., Percherancier, Y., Galandrin, S., Breit, A., Gales, C., Bouvier, M. Cholesterol-dependent separation of the beta2-adrenergic receptor from its partners determines signaling efficacy: Insight into nanoscale organization of signal transduction. *J. Biol. Chem.* 2008, 283, 24659–72.
4. Hurley, J.H., Misra, S. Signaling and subcellular targeting by membrane binding domains. *Annu. Rev. Biophys. Biomol. Struct.* 2000, 29, 49–79.
5. Lemon, M.A., Ferguson, K.M. Signal-dependent membrane targeting by pleckstrin homology (PH) domain. *Biochem. J.* 2000, 350, 1–18.
6. Hamada, K., Shimizu, T., Matsui, T., Tsukita, S., Hakoshima, T. Structural basis of the membrane-targeting and unmasking mechanisms of radixin FERM domain. *EMBO J.* 2000, 19, 4449–62.
7. Peter, B.J., Kent, H.M., Mills, I.G., Vallis, Y., Butler, P.J.G., Evans, P.R., McMahon, H.T. BAR domains as sensors of membrane curvature: The amphiphysin BAR structure. *Science* 2004, 303, 495–9.
8. Madsen, K.L., Eriksen, J., Milan-Lobo, L., Han, D.S., Niv, M.Y., Ammendrup-Johnsen, I., Henriksen, U., Bhatia, V.K., Stamou, D., Sitte, H.H., McMahon, H.T., Weinstein, H., Gether, U. Membrane localization is critical for activation of the PICK1 BAR (bin/amphiphysin/rvs) domain. *Traffic* 2008, 9, 1327–43.
9. Simons, K., Ikonen, E. Functional rafts in cell membranes. *Nature* 1997, 387, 569–72.
10. Brown, D.A. Lipid rafts, detergent-resistant membranes, and raft targeting signals. *Physiology* 2006, 21, 430–9.
11. Veatch, S.L., Keller, S.L. Seeing spots: Complex phase behavior in simple membranes. *Biochim. Biophys. Acta* 2005, 1746, 172–85.
12. Edidin, M. The state of lipid rafts: From model membranes to cells. *Annu. Rev. Biophys. Biomol. Struct.* 2003, 32, 257–83.

13. Munro, S. Lipid rafts: Elusive or illusive? *Cell* 2003, 115, 377–88.
14. Simons, K., Vaz, W.L. Model systems, lipid rafts, and cell membranes. *Annu. Rev. Biophys. Biomol. Struct.* 2004, 33, 269–95.
15. McMullen, T.P.W., Lewis, R.N.A.H., McElhane, R.N. Cholesterol–phospholipid interactions, the liquid-ordered phase and lipid rafts in model and biological membranes. *Curr. Opin. Colloid Interface Sci.* 2004, 8, 459–68.
16. Lichtenber, D., Goni, F.M., Heerklotz, H. Detergent-resistant membranes should not be identified with membrane rafts. *Trend. Biochem. Sci.* 2005, 30, 430–6.
17. Pandit, S.A., Khelashvili, G., Jakobsson, E., Grama, A., Scott, H.L. Lateral organization in lipid-cholesterol mixed bilayers. *Biophys. J.* 2007, 92, 440–7.
18. Khelashvili, G., Pandit, S.A., Scott, H.L. Self-consistent mean-field model based on molecular dynamics: Application to lipid-cholesterol bilayers. *J. Chem. Phys.* 2005, 123, 034910.
19. Khelashvili, G., Scott, H.L. Combined Monte Carlo and molecular dynamics simulation of hydrated 18:0 sphingomyelin-cholesterol lipid bilayers. *J. Chem. Phys.* 2004, 120, 9841–7.
20. Varma, R., Mayor, S. GPI-anchored proteins are organized in submicron domains at the cell surface. *Nature* 1998, 394, 798–801.
21. Friedrichson, T., Kurzchalia, T.V. Microdomains of GPI-anchored proteins in living cells revealed by crosslinking. *Nature* 1998, 394, 801–5.
22. Arkhipov, A., Yin, Y., Schulten, K. Four-scale description of membrane sculpting by BAR domains. *Biophys. J.* 2008, 95, 2806–21.
23. Marrink, S.J., Risselada, H.J., Yefimov, S., Tieleman, D.P., de Vries, A.H. The MARTINI force field: Coarse grained model for biomolecular simulations. *J. Phys. Chem. B* 2007, 111, 7812–24.
24. Lu, L., Voth, G.A. Systematic coarse-graining of a multicomponent lipid bilayer. *J. Phys. Chem. B* 2009, 113, 1501–10.
25. Ayton, G.S., Blood, P.D., Voth, G.A. Membrane remodeling from N-BAR domain interactions: Insights from multi-scale simulation. *Biophys. J.* 2007, 92, 3595–602.
26. Khelashvili, G., Weinstein, H., Harries, D. Protein diffusion on charged membranes: A dynamic mean-field model describes time evolution and lipid reorganization. *Biophys. J.* 2008, 94, 2580–97.
27. Khelashvili, G., Harries, D., Weinstein, H. Modeling membrane deformations and lipid demixing upon protein-membrane interaction: The BAR dimer adsorption. *Biophys. J.* 2009, 97, 1626–35.
28. Chaikin, P.M., Lubensky, T.C. *Principles of Condensed Matter Physics*, Cambridge University Press, Cambridge, 2000.
29. Helfrich, W. Elastic properties of lipid bilayers: Theory and possible experiments. *Z. Naturforsch.* 1973, 28c, 693–703.
30. Sharp, K.A., Honig, B. Electrostatic interactions in macromolecules: Theory and applications. *Annu. Rev. Biophys. Chem.* 1990, 19, 301–32.
31. Andelman, D. In *Handbook of Biological Physics* (eds A.J. Hoff), Vol. 1B, Elsevier Science B.V., Amsterdam, 1995, pp. 603–42.
32. Reiner, E.S., Radke, C.J. Variational approach to the electrostatic free energy in charged colloidal suspensions: General theory for open systems. *J. Chem. Soc. Faraday Trans.* 1990, 86, 3901–12.
33. Honig, B., Nicholls, A. Classical electrostatics in biology and chemistry. *Science* 1995, 268, 1144–9.
34. Borukhov, I., Andelman, D., Orland, H. Steric effects in electrolytes: A modified Poisson-Boltzmann equation. *Phys. Rev. Lett.* 1997, 79, 435–8.
35. Fogolari, F., Briggs, J.M. On the variational approach to the Poisson-Boltzmann free energies. *Chem. Phys. Lett.* 1997, 281, 135–9.
36. Harries, D., May, S., Ben-Shaul, A. Curvature and charge modulations in lamellar DNA-lipid complexes. *J. Phys. Chem. B* 2003, 107, 3624–30.
37. Chernomordik, L.V., Kozlov, M.M. Protein-lipid interplay in fusion and fission of biological membranes. *Annu. Rev. Biochem.* 2003, 72, 175–207.
38. Jahn, R., Grubmüller, H. Membrane fusion. *Curr. Opin. Cell Biol.* 2002, 14, 488–95.
39. Kozlovsky, Y., Efrat, A., Siegel, D.A., Kozlov, M.M. Stalk phase formation: Effects on dehydration and saddle splay modulus. *Biophys. J.* 2004, 87, 2508–21.
40. Kozlovsky, Y., Kozlov, M.M. Membrane fission: Model for intermediate structures. *Biophys. J.* 2003, 85, 85–96.
41. Wiese, W., Helfrich, W. Theory of vesicle budding. *J. Phys. Condens. Matter* 1990, 2, SA329–32.

42. Mashl, R.J., Bruinsma, R.F. Spontaneous-curvature theory of clathrin-coated membranes. *Biophys. J.* 1998, 74, 2862–75.
43. May, S., Harries, D., Ben-Shaul, A. Lipid demixing and protein-protein interactions in the adsorption of charged proteins on mixed membrane. *Biophys. J.* 2000, 79, 1747–60.
44. Harries, D., May, S., Gelbart, W.M., Ben-Shaul, A. Structure, stability, and thermodynamics of lamellar DNA-lipid complexes. *Biophys. J.* 1998, 75, 159–73.
45. Haleva, E., Ben-Tal, N., Diamant, H. Increased concentration of polyvalent phospholipids in the adsorption domain of a charged protein. *Biophys. J.* 2004, 86, 2165–78.
46. Wang, J., Gambhir, A., McLaughlin, S., Murray, D.A. Computational model for the electrostatic sequestration of PI(4,5)P₂ by membrane-adsorbed based peptides. *Biophys. J.* 2004, 86, 1969–86.
47. McLaughlin, S., Murray, D. Plasma membrane phosphoinositide organization by protein electrostatics. *Nature* 2005, 438, 605–11.
48. Andelman, D., Kozlov, M.M., Helfrich, W. Phase transitions between vesicles and micelles driven by competing curvature. *Europhys. Lett.* 1994, 25, 231–6.
49. Petrache, H.I., Harries, D., Parsegian, V.A. Alteration of lipid membrane rigidity by cholesterol and its metabolic precursors. *Macromol. Symp.* 2005, 219, 39–50.
50. Petrache, H.I., Gouliaev, N., Tristram-Nagle, S., Zhang, R.T., Sutter, R.M., Nagle, J.F. Interbilayer interactions from high-resolution x-ray scattering. *Phys. Rev. E* 1998, 57, 7014–24.
51. Evans, E.A., Parsegian, V.A. Thermal-mechanical fluctuations enhance repulsion between biomolecular layers. *Proc. Natl. Acad. Sci.* 1986, 83, 7132–6.
52. Podgornik, R., Parsegian, V.A. Thermal-mechanical fluctuations of fluid membranes in confined geometries: The case of soft confinement. *Langmuir* 1992, 8, 557–62.
53. Fang, F., Szleifer, I. Competitive adsorption in model charged protein mixtures: Equilibrium isotherms and kinetic behavior. *J. Chem. Phys.* 2003, 119, 1053–65.
54. Fang, F., Szleifer, I. Controlled release of proteins from polymer-modified surfaces. *Proc. Natl. Acad. Sci.* 2006, 103, 5769–74.
55. Faure, M.C., Bassereau, P., Carignao, M.A., Szleifer, I., Gallot, Y., Andelman, D. Monolayers of diblock copolymer at the air-water interface: The attractive monomer-surface case. *Euro. Phys. J. B* 1998, 3, 365–75.
56. Saxton, M. Anomalous diffusion due to binding: A Monte Carlo study. *Biophys. J.* 1996, 70, 1250–62.
57. Binder, K., Heermann, D.W. *Monte Carlo Simulation in Statistical Physics*, Springer Verlag, Berlin, 2002.
58. Fichtorn, K.A., Weinberg, W.H. Theoretical foundations of dynamical Monte Carlo simulations. *J. Chem. Phys.* 1991, 95, 1090–6.
59. Kang, H.C., Weinberg, W.H. Monte Carlo simulations of surface-rate processes. *Acc. Chem. Res.* 1992, 25, 253–9.
60. Baumgartner, A. Statics and dynamics of the freely jointed polymer chain with Lennard-Jones interaction. *J. Chem. Phys.* 1980, 72, 871–9.
61. Graf, P., Nitzan, A., Kurnikova, M.G., Coalson, R.D. A dynamic lattice Monte Carlo model of ion transport in inhomogeneous dielectric environments: Method and implementation. *J. Phys. Chem. B* 2000, 104, 12324–38.
62. Chern, S.-S., Cardenas, A.E., Coalson, R.D. Three-dimensional dynamic Monte Carlo simulations of driven polymer transport through a hole in a wall. *J. Chem. Phys.* 2001, 115, 7772–82.
63. Campelo, F., McMahon, H.T., Kozlov, M.M. The hydrophobic insertion mechanism of membrane curvature generation by proteins. *Biophys. J.* 2008, 95, 2325–39.
64. Zemel, A., Ben-Shaul, A., May, S. Perturbation of a lipid membrane by amphiphatic peptides and its role in pore formation. *Biophys. J.* 2005, 88, 230–42.
65. McLaughlin, S., Wang, J., Gambhir, A., Murray, D. PIP₂ and proteins: Interactions, organization, and information flow. *Annu. Rev. Biophys. Struct.* 2002, 31, 151–75.
66. McLaughlin, S., Murray, D. Plasma membrane phosphoinositide organization by protein electrostatics. *Nature* 2005, 438, 605–11.
67. Heo, W.D., Inoue, T., Park, W.S., Kim, M.L., Park, B.O., Wandless, T.J., Meyer, T. PI(3,4,5)P₃ and PI(4,5)P₂ lipids target proteins with polybasic clusters to the plasma membrane. *Science* 2006, 314, 1458–61.

68. Yeung, T., Terebiznik, M., Yu, L., Silvius, J., Abidi, W.M., Phillips, M., Levine, T., Kapus, A., Grinstein, S. Receptor activation alters inner surface potential during phagocytosis. *Science* 2006, 313, 347–51.
69. Wang, J., Gambhir, A., Hangyas-Mihalyne, G., Murray, D., Golebiewska, U., McLaughlin, S. Lateral sequestration of phosphatidylinositol 4,5-bisphosphate by the basic effector domain of myristoylated alanine-rich C kinase substrate is due to nonspecific electrostatic interactions. *J. Biol. Chem.* 2002, 277, 34401–12.
70. Nomikos, M., Mulgrew-Nesbitt, A., Pallavi, P., Mihalyne, G., Zaitseva, I., Swann, K., Lai, F.A., Murray, D., McLaughlin, S. Binding of phosphoinositide-specific phospholipase C- ζ (PLC- ζ) to phospholipid membranes: Potential role of an unstructured cluster of basic residues. *J. Biol. Chem.* 2007, 282, 16644–53.
71. Golebiewska, U., Gambhir, A., Hangyas-Mihalyne, G., Zaitseva, I., Radler, J., McLaughlin, S. Membrane-bound basic peptides sequester multivalent (PIP₂), but not monovalent (PS), acidic lipids. *Biophys. J.* 2006, 91, 588–99.
72. Tzllil, S., Ben-Shaul, A. Flexible charged macromolecules on mixed fluid lipid membranes: Theory and Monte-Carlo simulations. *Biophys. J.* 2004, 89, 2972–87.
73. Wang, J., Gambhir, A., McLaughlin, S., Murray, D. A computational model for the electrostatic sequestration of PI(4,5)P₂ by membrane-adsorbed based peptides. *Biophys. J.* 2004, 86, 1969–86.
74. Gomperts, B., Tatham, P., Kramer, I. *Signal Transduction*, Academic Press, San Diego, 2003.
75. Record, M.T. Jr., Anderson, C.F., Lohman, T.M. Thermodynamic analysis of ion effects on the binding and conformational equilibria of proteins and nucleic acids: The roles of ion association or release, screening, and ion effects on water activity. *Q. Rev. Biophys.* 1978, 11, 103–78.
76. Parsegian, V.A., Gingell, D. On the electrostatic interaction across a salt solution between two bodies bearing unequal charges. *Biophys. J.* 1972, 81, 1192–204.
77. Wagner, K., Harries, D., May, S., Kahl, V., Raedler, J.O., Ben-Shaul, A. Direct evidence for counterion release upon cationic lipid-DNA condensation. *Langmuir* 2000, 16, 303–6.
78. Sharp, K.A., Friedman, R.A., Misra, V., Hecht, J., Honig, B. Salt effects on polyelectrolyte-ligand binding: Comparison of Poisson-Boltzmann, and limiting law/counterion binding models. *Biopolymers* 1995, 36, 245–62.
79. Ren, G., Vajjhala, P., Lee, J.S., Winsor, B., Munn, A.L. The BAR domain proteins: Molding membranes in fission, fusion, and phagy. *Microbiol. Mol. Biol. Rev.* 2006, 70, 37–120.
80. Habermann, B. The BAR-domain family of proteins: A case of bending and binding? *EMBO Rep.* 2004, 5, 250–5.
81. Dawson, J.C., Legg, J.A., Machesky, L.M. BAR domain proteins: A role in tubulation, scission and actin assembly in clathrin-mediated endocytosis. *Trends. Cell Biol.* 2006, 16, 493–8.
82. Perez, J.L., Khatri, L., Chang, C., Srivastava, S., Osten, P., Ziff, E.B. PICK1 targets activated protein kinase calpha to AMPA receptor clusters in spines of hippocampal neurons and reduces surface levels of the AMPA-type glutamate receptor subunit 2. *J. Neurosci.* 2001, 21, 5417–28.
83. Lu, W., Ziff, E.B. PICK1 interacts with ABP/GRIP to regulate AMPA receptor trafficking. *Neuron* 2005, 47, 407–21.
84. Jin, W., Ge, W.-P., Xu, J., Cao, M., Peng, L., Yung, W., Liao, D., Duan, S., Zhang, M., Xia, J. Lipid binding regulates synaptic targeting of PICK1, AMPA receptor trafficking, and synaptic plasticity. *J. Neurosci.* 2006, 26, 2380–90.
85. Saarikangas, J., Zhao, H., Pykalainen, A., Laurinmaki, P., Mattila, P.K., Kinnunen, P.K., Butcher, S.J., Lappalainen, P. Molecular mechanisms of membrane deformation by I-BAR domain proteins. *Curr. Biol.* 2009, 19, 95–107.
86. Gallop, J.L., McMahon, H.T. BAR domains and membrane curvature: Bringing your curves to the BAR. *Biochem. Soc. Symp.* 2005, 72, 223–31.
87. Itoh, T., De Camilli, P. BAR, F-BAR (EFC) and ENTH/ANTH domains in the regulation of membrane-cytosol interfaces and membrane curvature. *Biochim. Biophys. Acta* 2006, 1761, 897–912.
88. Zimmerberg, J., Kozlov, M.M. How proteins produce cellular membrane curvature. *Nat. Rev. Mol. Cell. Biol.* 2006, 7, 9–19.
89. Gallop, J.L., Jao, C.C., Kent, H.M., Butler, P.J.G., Evans, P.R., Langen, R., McMahon, H.T. Mechanism of endophilin N-BAR domain-mediated membrane curvature. *EMBO J.* 2004, 25, 2898–910.

90. Farsad, K., Ringstad, N., Takei, K., Floyd, S.R., Rose, K., De Camilli, P. Generation of high curvature membranes mediated by direct endophilin bilayer interactions. *J. Cell. Biochem.* 2001, 155, 193–200.
91. Masuda, M., Takeda, S., Sone, M., Ohki, T., Mori, H., Kamioka, Y., Mochizuki, N. Endophilin BAR domain drives membrane curvature by two newly identified structure-based mechanisms. *EMBO J.* 2006, 25, 2889–97.
92. Ford, M.G.J., Mills, I.G., Peter, B.J., Valls, Y., Praefcke, G.J.K., Evans, P.R., McMahon, H.T. Curvature of clathrin-coated pits driven by epsin. *Nature* 2002, 419, 361–6.
93. Lee, M.C., Orci, L., Hamamoto, S., Futral, E., Ravazzola, M., Schekman, R. Sar1p N-terminal helix initiates membrane curvature and completes the fission of a COPII vesicle. *Cell* 2005, 122, 605–17.
94. Nie, Z., Hirsch, D.S., Luo, R., Jian, X., Stauffer, S., Cremesti, A., Andrade, J., Lebowitz, J., Marino, M., Ahvazi, B., Hinshaw, J.E., Randazzo, P.A. A BAR domain in the N terminus of the arf GAP ASAP1 affects membrane structure and trafficking of epidermal growth factor receptor. *Curr. Biol.* 2006, 16, 130–9.
95. Fernandes, F., Loura, L.M.S., Chichon, F.J., Carrascosa, J.L., Fedorov, A., Prieto, M. Role of helix-0 of the N-BAR domain in membrane curvature generation. *Biophys. J.* 2008, 94, 3065–73.
96. Baker, N.A., Sept, D., Joseph, S., Holst, M.J., McCammon, J.A. Electrostatics of nanosystems: Application to microtubules and the ribosome. *Proc. Natl. Acad. Sci.* 2001, 98, 10037–41.
97. Lindahl, E., Edholm, O. Mesoscopic undulations and thickness fluctuations in lipid bilayers from molecular dynamics simulations. *Biophys. J.* 2000, 79, 426–33.
98. Ayton, G.S., Lyman, E., Krishna, V., Swenson, R.D., Mim, C., Unger, V.M., Voth, G.A. New insights into BAR domain-induced membrane remodeling. *Biophys. J.* 2009, 97, 1616–25.
99. Yin, Y., Arikhipov, A., Schulten, K. Simulations of membrane tubulation by lattices of amphiphysin N-BAR domains. *Structure* 2009, 17, 882–92.
100. Frost, A., Perera, R., Roux, A., Spasov, K., Destaing, O., Egelman, E.H., de Camilli, P., Unger, V.M. Structural basis of membrane invagination by F-BAR domains. *Cell* 2008, 132, 807–17.
101. Shimada, A., Niwa, H., Tsujita, K., Suetsugu, S., Nitta, K., Hanawa-Suetsugu, K., Akasaka, R., Nishino, Y., Toyama, M., Chen, L., Liu, Z.-J., Wang, B.-C., Yamamoto, M., Terada, T., Miyazawa, A., Tanaka, A., Sugano, S., Shirouzu, M., Nagayama, J., Takenawa, T., Yokoyama, S. Curved EFC/F-BAR-domain dimers are joined end to end into a filament for membrane invagination in endocytosis. *Cell* 2007, 129, 761–72.